Energy Systems
https://doi.org/10.1007/s12667-021-00437-9

ORIGINAL PAPER

Investigating the impact of stochasticity in microgrid energy management

Amelia McIlvenna[1] · **Ben Ollis**[2] · **James Ostrowski**[1]

Received: 14 January 2020 / Accepted: 3 April 2021

Abstract

Various stochastic programming methods have been used to account for penetration of uncertain renewable energy generation in microgrids. However, these stochastic methods may be unnecessary. Energy storage combined with rescheduling based on a rolling time horizon gives a microgrid powerful tools to adapt to any unexpected events. Add to that the natural tendency to over-engineer new systems and one begins to wonder how much value can be gained by stochastic optimization over deterministic methods. We investigated this question by looking at an existing residential microgrid in Hoover, AL. We compare various stochastic approaches for scheduling with deterministic approaches and show that there is little value of using stochastic programming. Instead, we find that considering longer time horizons is a better use of computational resources.

Keywords Microgrids · Stochastic programming · Energy management system · Rolling horizon

✉ James Ostrowski
jostrows@utk.edu

Amelia McIlvenna
amcilven@vols.utk.edu

[1] Industrial and Systems Engineering, University of Tennessee, Knoxville, TN 37996, USA

[2] Oak Ridge National Laboratory, Oak Ridge, TN 37830, USA

Published online: 13 April 2021

Abbreviations

Variables

u_{gt}^{s}	Commitment status for each generator g in time t, for scenario s, $\in \{0, 1\}$
v_{gt}^{s}	Generator start up indicator for each generator g in time t, scenario s $\in \{0, 1\}$
u_{bt}^{Cs}, u_{bt}^{Ds}	Battery charging/discharging status, respectively in time t, scenario s, $\in \{0, 1\}$
P_{gt}^{s}	Total power (kW) at each generator g in time t, for scenario s, $\in \mathbb{R}^{+}$
P_{bt}^{Cs}, P_{bt}^{Ds}	Battery charging/discharging power (kW), respectively, $\in \mathbb{R}^{+}$
p_{gt}^{ms}	Power at mth generator interval (kW), $\in \mathbb{R}^{+}$
P_{vt}^{s}	PV power which is not curtailed at time t, scenario s (kW), $\in \mathbb{R}^{+}$
E_{bt}^{s}	Energy in battery b at time t for scenario s (kWh), $\in \mathbb{R}^{+}$
$E_{bt}^{EX,s}$	Amount of battery extreme energy in time t, scenario s (kWh), $\in \mathbb{R}^{+}$
P_{bt}^{Vs}	Difference in battery power between time t and $t-1$, scenario s, $\in \mathbb{R}$
L_{t}^{s}	Load shed at time t scenario s, $\in \mathbb{R}^{+}$

Parameters

k_{g}	minimum up cost of generator g
C_{gt}^{m}	Marginal cost for mth generator interval (strictly increasing)
C_{gt}^{v}	Start up cost for generator g
C_{bt}	Battery operational cost
η_{b}^{C}	Charging efficiency of battery b
η_{b}^{D}	Discharging efficiency of batter b
P_{g}^{min}	Generator min up power
$P_{b,INIT}$	Initial power output of battery b
D_{t}	Real demand at time t
P_{vt}^{Fs}	Forecasted PV power at time t for scenario s
E_{b}^{min}	Minimum allowable energy for battery b
E_{b}^{max}	Maximum allowable energy for battery b
E_{b}^{cap}	Maximum energy capacity for battery b
$E_{b,INIT}$	Initial state of charge of batter b
TU_{g}	Minimum up-time for generator g

Sets

$g \in \mathcal{G}$	Set of generators
$b \in \mathcal{B}$	Set of batteries
$v \in \mathcal{V}$	Set of PV panels
$m \in \mathcal{I}$	Set of piecewise generator power components
$t \in \mathcal{T}$	Set of timeperiods
$s \in \mathcal{S}$	Set of scenarios

1 Introduction

Due to deregulation of electricity markets and increasing renewable energy adoption, distributed electricity generation is gaining traction. Microgrids have been introduced as a way to facilitate distributed energy and incorporate renewables while improving reliability [1]. Microgrids have already shown promise in delivering power to remote areas, as well as the ability to coexist with existing electrical infrastructure [2, 3].

because of their distributed nature, microgrids require local control and optimization infrastructure to ensure successful operation, especially when isolated from any other electrical grid [4]. Many deterministic and stochastic optimization architectures have been developed to handle this need for local optimization of assets [5, 6]. The stochastic methods have the advantage of accounting for uncertain quantities in their operation such as wind turbines, photovoltaic (PV) power, and load. On the other hand, stochastic optimization often requires decomposition algorithms due to the large size of the models.

Widely used decomposition schemes include L-shaped methods [7, 8], which use a cutting plane technique to achieve an optimal solution. Progressive hedging is another decomposition method which has been successfully used to solve mixed-integer stochastic programs [9]. Lagrangian-based methods are also effective, such as the dual decomposition algorithm [10], and the diagonal quadratic approximation method[11]. While decomposition methods are quite useful in solving large problems, they may be hard to implement in practice within a microgrid controls architecture as solutions are required quickly and the controller may not have access to commercial optimization software. Many decomposition schemes require multiple time-intensive iterations, or are decomposed in such a way to facilitate parallel computation which may not be possible in a hardware-limited environment.

In [12], a two-stage stochastic program was formulated for a microgrid system with connection to the main grid, where the second stage included optimal power flow for both the main and micro grids. Another two-stage stochastic program for microgrid operation was developed in [13] and solved via an adaptive modified firefly algorithm.

An additional emphasis on reliability can be incorporated by adding measures of robustness or risk-aversion into the model [14]. A risk-averse two-stage stochastic UC model was presented in [15] which uses a CvaR asessment to quantify risk for isolated microgrids. A CvaR assesment is also analyzed in [16] for unexpected islanding events where the microgrid is rendered isolated.

Coupling stochastic generation with demand response has also been explored in the literature [17, 18]. A stochastic formulation for a microgrid with uncertain wind and PV was simulated with and without demand response in [19]. Using a bender's decomposition with second stage power flow constraints, it was found that demand response provided further benefits in cost reduction than the stochastic formulation alone.

Many isolated microgrids operate with a fixed forecast horizon of 24–48 h. A recent forecast horizon model was examined in [20], which can be useful for

microgrids in the event that information may not always be available for a complete forecast 24–48 h forecast horizon. In [21] a two-stage stochastic model for microgrid energy scheduling with grid connection was developed. The model also showed reduction in operational cost and power losses when compared to its deterministic equivalent.

For microgrids which are operating under real-time conditions, rolling horizon models can help account for some uncertainty by extending the forecast horizon and re-solving for device setpoints throughout the day. A deterministic rolling horizon model for an existing microgrid in Chile was developed in [22]. This deterministic rolling horizon model showed overall lower cost compared to a day-ahead unit commitment model. Noticeably lacking in the literature is consideration of two-stage stochastic microgrid optimization under a rolling time horizon. There has been one attempt at such a model in [23], which modified a deterministic rolling time mixed-integer linear program (MILP) from [24] to account for uncertain heat and energy demand as well as wind power generation. The stochastic model incorporated a prediction horizon of k hours for which all scenarios were considered equal in order to extract a controls schedule for the generation devices and scheduling of tasks within residential homes. The time periods considered in [23], however, were 30 minutes long with forecasts considered deterministic during a lengthy prediction horizon. While this may be necessary for microgrids with ramping restrictions, for those with no restriction (such as the microgrid in this study) it is possible to solve for both commitment and dispatch decisions and deploy them for time intervals much shorter than 30 minutes in length. Solving the model using shorter time intervals can make better use of new information as uncertainties are realized. This is because the model can incorporate measured values for uncertain quantities more frequently, thereby leading to more frequent adjustments of operational setpoints that may have turned out to be sub-optimal.

This study develops a two-stage rolling time horizon stochastic programming model for an existing microgrid located in Hoover, Alabama. The microgrid serves a residential neighborhood of approximately 60 homes, and was the first of its kind constructed in the southeastern U.S. [25]. As a result of the Hoover microgrid's small size, we employ 5-minute time intervals for a 24-h forecast horizon, and a unique stage formulation broken by time intervals which helps to maximize the amount of uncertainty accounted for in the model. Currently the microgrid is operated using a 5-minute deterministic rolling time horizon optimization which delivers dispatch setpoints to the devices in the microgrid. These devices are comprised of a natural gas generator, PV system, and a lithium-ion battery. The Hoover microgrid has grid connection capabilities, however we will assume the microgrid is in island mode (i.e. isolated) for this study, as this is the most critical operational configuration. A deterministic MILP which uses a relaxation technique to improve solution time has already been developed for this microgrid [26].

We will describe a rolling time stochastic model formulation looks like in Sect. 2. Then, Sect. 3 will detail computational results from a variety of test cases using real-world data from the existing Hoover microgrid. Both forecasted values and measured data for the PV system was collected under real-time operation of the microgrid. In addition, real-time measured values for residential neighborhood demand

were collected and used for the demand values in the computational results. Lastly, Sect. 4 will conclude the discussion. We then investigate the value gained from stochastic approaches and give evidence that longer time horizons are likely to be more important than considering uncertainty.

2 Model

We will now construct our stochastic model formulation for the Hoover microgrid. For any two-stage stochastic problem, it must be determined which variables will belong to the first and second stage. Traditionally in power systems problems, generator commitment and start-up variables ($u_{g,t}, v_{g,t}$) would be included in the first stage, as commitment is often decided on a day-ahead basis. But this microgrid can ramp up any generation device within a 5-minute window, as the generator has a maximum power of only 400kW. Because of the fast ramping capabilities it is not necessary to decide commitment ahead of time. We can therefore decide these commitment variables as we roll through the day, meaning we only need to know the value of the commitment variables at present time. What becomes more important is to be able to extract valid setpoints for all devices in the microgrid from the solution of the optimization even though it is a stochastic formulation. Setting up the problem with multiple scenarios at every time period would make it difficult to determine valid power setpoints, as the time period corresponding to present time would have variables for each scenario.

In [23] this issue of extracting device setpoints is handled by setting all scenarios equal for a certain prediction horizon near in the future. Instead of adopting a similar framework, we take a novel approach of breaking first and second stage variables by time interval instead of variable type. We will let all variables associated with the first time period $t = 0$ belong in the first stage. All variables not in the first time period (i.e. $t = 1, 2, \cdots 287$) will be the second stage. A breakdown of the stages and the most crucial variables in each is shown in Fig. 1. With the stages constructed in this manner the first time period will have unique variables for each power setpoint and/or commitment status needed. Then because the first time period $t = 0$

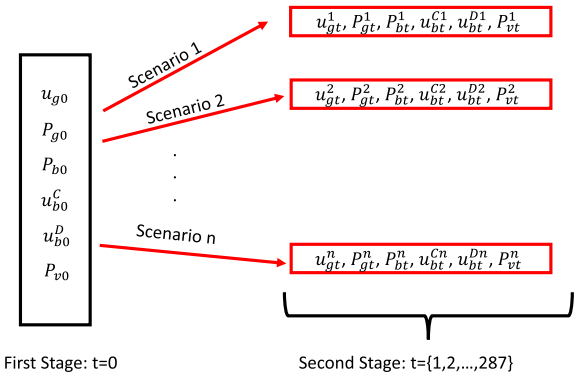

Fig. 1 Stage Construction for the stochastic program broken by time interval with important variables listed for each stage

will always represent the present time, these setpoint values can be delivered to the devices in the microgrid, and the current cost of operation can be calculated.

It is important to note that breaking stages by time period will leave the second stage with integer variables. For microgrids with a large number of assets these variables would necessitate advanced techniques for obtaining a solution. Fortunately the microgrid in this study is small, and with only one generator, battery, and PV system, the stochastic formulation is still small enough to be solved in its extensive form within the required 5-minute time frame for almost all instances (a fact we will revisit in Sect. 3). Therefore we do not need to worry about including commitment variables in the second stage.

To formulate the model, we start with the objective (1) which will minimize cost of operation for the microgrid. Because the first stage includes variables which represent the present time, the first stage cost will be the generator and battery costs at $t = 0$, plus the penalty terms represented by β. The generator cost is represented as a piecewise approximation of a convex quadratic cost curve. Therefore the marginal costs for each generator can be represented by a set of strictly increasing piecewise power production costs C_g^m, with corresponding power production levels p_{gt}^m. PV is assumed to have negligible cost. Second stage cost for each scenario includes cost for generator and battery operation in time periods $t = \{1, 2, \cdots, 287\}$ along with penalty terms represented by δ. We assume a finite number of scenarios. The total second stage cost is represented by its expected value, which is the summation of each scenario's cost multiplied by the corresponding probability $prob_s$.

$$\begin{aligned}
\min \; & \sum_{g\in\mathcal{G}} \left[k_g u_{g0} + C_g^{SU} v_{g0}\right] \\
& + \sum_{g\in\mathcal{G}} \sum_{m\in\mathcal{I}} C_g^m p_{g0}^m + \sum_{b\in\mathcal{B}} C_{b0}(P_{b0}^D + P_{b0}^C) + \beta \\
& + \sum_{s\in\mathcal{S}} prob_s \Bigg(\sum_{t\in\mathcal{T}} \sum_{g\in\mathcal{G}} \left[k_g u_{gt} + C_g^{SU} v_{gt}\right] \\
& + \sum_{t\in\mathcal{T}} \sum_{g\in\mathcal{G}} \sum_{m\in\mathcal{I}} C_g^m p_{gt}^m + \sum_{t\in\mathcal{T}} \sum_{b\in\mathcal{B}} C_{bt}\left(P_{bt}^D + P_{bt}^C\right) + \delta \Bigg)
\end{aligned} \tag{1}$$

Penalty terms which penalize undesirable behavior for both the first and second stage are detailed in (2) and (3), respectively. In (2), β_E is the penalty parameter for extreme state of charge of the battery E_{b0}^{EX} at time period 0, while β_V is the penalty parameter for the difference in battery power between the first time interval and the initial battery power, represented by $P_{b,0}^V$. The bounds on these variables are detailed later in equations (5g)-(5j). The parameters δ_E and δ_B are similar to β_E and β_V, but penalize all time periods which occur in the second stage.

$$\beta = \beta_E \cdot \sum_{b\in\mathcal{B}} E_{b0}^{EX} + \beta_V \cdot \sum_{b\in\mathcal{B}} P_{b0}^V \tag{2}$$

$$\delta = \delta_E \cdot \sum_{t\in\mathcal{T}} \sum_{b\in\mathcal{B}} E^{EX}_{bt} + \delta_V \cdot \sum_{t\in\mathcal{T}} \sum_{b\in\mathcal{B}} P^{V}_{bt} \tag{3}$$

2.1 Constraints

First we will introduce the first-stage constraints, which represent all operational constraints for time period $t = 0$. Constraint (4a) sets total generator power at time 0, P_{g0}, equal to the sum of its piecewise power components, which are bounded in (4b). Let u_g^{INIT} be the initial commitment status of the generator. Then constraint (4c) represents the generator start up status at time $t = 0$, denoted v_{g0}, where u_{g0} will be the generator's commitment status. Constraint (4d) bounds the total power output of the generator.

$$P_{g0} = \sum_{i\in\mathcal{I}} p^m_{g0} + u_{g0} P^{min}_g \tag{4a}$$

$$0 \le p^m_{g0} \le p^{max,m}_{g0} u_{g0} \quad \forall\, m \in \mathcal{I} \tag{4b}$$

$$u_{g0} - u_{g,INIT} \le v_{g0} \tag{4c}$$

$$\begin{gathered} 0 \le P_{g0} \le P^{max}_{g0} u_{g0} \\ \forall g \in \mathcal{G} \end{gathered} \tag{4d}$$

For the battery, we bound its charging rate P^C_{b0}, and discharging rate P^D_{b0} at time 0 in (5a),(5b). The battery is restricted to be either charging or discharging at time 0 in (5c). Energy in the battery at time 0 is modeled by (5d), where E^{INIT}_b is the initial energy in the battery, η^C_b and η^D_b are the charging and discharging efficiencies respectively, and δ_t is the length of one time interval expressed as a fraction of an hour. Energy capacity E_{b0} is bounded in (5e), with E^{cap}_b as the maximum capacity of energy in the battery. For simplicity in notation, we set the total signed power in the battery as (5f).

Constraints (5g) and (5h) keep track of the difference in battery power from the initial power output $P_{b,INIT}$ and the first time interval. This difference, represented by P^V_{b0}, is penalized in (2). While these constraints initially seem obscure, they are included as a means to minimize unnecessary cycling of the battery in the Hoover microgrid, by attempting to avoid drastic changes in the battery power setpoint. By minimizing unnecessary cycling, we discourage situations in which the battery will cycle frequently, under-utilizing its storage capacity [27].

We also wish to avoid fully charging or discharging the battery, as it has been shown that this behavior will shorten its operational lifetime [27]. We can define an acceptable maximum state of charge (SOC) which is less than the battery's capacity, and a minimum SOC which is greater than 0. The battery is considered to be in an extreme state of charge if its energy is above the acceptable maximum E^{max}_b or below the acceptable minimum E^{min}_b, with $0 < E^{min}_b < E^{max}_b < E^{cap}_b$. Constraints (5i) and (5j) will induce

a penalty in (2) if the battery enters an extreme state of charge in the first stage. The energy quantity which is either above the acceptable maximum or below the acceptable minimum is represented by E_{b0}^{EX}. This way, if an extreme SOC is necessary because of feasibility or an unexpected event occurs, the battery may assume this SOC for a penalty, and then will be motivated to either charge/discharge to a normal state of operation.

$$0 \leq P_{b0}^{C} \leq P_{b0}^{C,max} u_{b0}^{C} \tag{5a}$$

$$0 \leq P_{b0}^{D} \leq P_{b0}^{D,max} u_{b0}^{D} \tag{5b}$$

$$u_{b0}^{C} + u_{b0}^{D} \leq 1 \tag{5c}$$

$$E_{b0} = E_{b}^{INIT} + P_{b0}^{C} \eta_{b}^{C} \Delta t - P_{b0}^{D} \frac{1}{\eta_{b}^{D}} \Delta t \tag{5d}$$

$$0 \leq E_{b0} \leq E_{b}^{cap} \tag{5e}$$

$$P_{b0} = P_{b0}^{D} - P_{b0}^{C} \tag{5f}$$

$$P_{b0} - P_{b,INIT} \leq P_{b0}^{V} \tag{5g}$$

$$P_{b,INIT} - P_{b0} \leq P_{b0}^{V} \tag{5h}$$

$$E_{b}^{min} - E_{b0} \leq E_{b0}^{EX} \tag{5i}$$

$$E_{b0} - E_{b}^{max} \leq E_{b0}^{EX} \qquad \forall b \in \mathcal{B} \tag{5j}$$

Equation (6) balances energy production with demand D_0 at the present time, which accounts for only the first time period in the formulation. The variable L_0 accounts for load shedding at the first time period. The constraint (7) allows for PV curtailment less than its measured value P_{vt}^{MEAS}. Note that we are using the measured PV power instead of the forecasted PV power because we are at the present time as this quantity is realized.

$$\sum_{g \in \mathcal{G}} P_{g0} + \sum_{b \in \mathcal{B}} P_{b0} + \sum_{v \in \mathcal{V}} P_{v0} = D_0 - L_0 \tag{6}$$

$$P_{v0} \leq P_{v0}^{MEAS} \qquad \forall v \in \mathcal{V} \tag{7}$$

Now we will describe the second stage constraints, which account for each scenario $s \in \mathcal{S}$. Recall the second stage includes variables for all time periods $t \in \mathcal{T} \setminus 0$. Additionally, note if $t = 1$, then $u^s_{g,t-1} = u_{g0}\ \forall s \in \mathcal{S}$, because u_{g0} is a first stage variable. Then the generator constraints (8) are similar to those of (4) except they are designated for each scenario.

$$P^s_{gt} = \sum_{m \in \mathcal{I}} p^{sm}_{gt} + u_{gt} P^{min}_g \tag{8a}$$

$$0 \leq p^{ms}_{gt} \leq p^{max,m}_{gt} u^s_{gt} \quad \forall\, m \in \mathcal{I} \tag{8b}$$

$$u^s_{gt} - u^s_{g,t-1} \leq v^s_{gt} \tag{8c}$$

$$0 \leq P^s_{gt} \leq P^{max}_{gt} u^s_{gt} \qquad \forall g \in \mathcal{G}, t \in \mathcal{T} \setminus 0, s \in \mathcal{S} \tag{8d}$$

In large scale power systems problems, generators are typically modeled with a minimum up-time, that is, time for which, if a generator is turned in, it must stay on. While these constraints may not be physically necessary microgrids with a small generator such as the one in the Hoover microgrid, these constraints are included to discourage frequent generator cycling which can shorten the lifespan of the device. These constraints are described in (9a, 9b). Define the minimum up-time for the generator as TU, which is the minimum number of time intervals that the generator must be on for after started. Before forming the minimum up-time constraints, we need to consider whether the generator is currently on, and how long it has been operating for. This is important because the time horizon is rolling, so we cannot start from scratch each time the optimization is run. We let the quantity *uptimes* be equal to the number of time intervals left for which the generator must be on if it has been running for less than its minimum up-time at the present time. Note that if the generator was either off or on for more than the minimum up time before the first time interval, $uptimes = 0$. Also note that for brevity constraints () contain variables denoted per scenario, but in the case $t = 0$ we have only u_{g0}, v_{g0} as these are first stage variables.

$$u^s_{gt} = 1 \quad t < uptimes,\ t \in \mathcal{T}, s \in \mathcal{S} \tag{9a}$$

$$\sum_{i=t-TU_g+1}^{t} v^s_{gi} \leq u^s_{gt} \quad t \in \mathcal{T},\ s \in \mathcal{S} \tag{9b}$$

Constraints (10) constrain the battery in the second stage for all scenarios $s \in \mathcal{S}$. They are similar to constraints (5) but are formed on a per-scenario basis for all time periods in the second stage.

$$0 \leq P_{bt}^{Cs} \leq P_{bt}^{C,max} u_{bt}^{C} \tag{10a}$$

$$0 \leq P_{bt}^{Ds} \leq P_{bt}^{D,max} u_{bt}^{D} \tag{10b}$$

$$u_{bt}^{C} + u_{bt}^{D} \leq 1 \tag{10c}$$

$$E_{bt}^{s} = E_{b,t-1}^{s} + P_{bt}^{Cs} \eta_{b}^{C} \Delta t - P_{bt}^{Ds} \frac{1}{\eta_{b}^{D}} \Delta t \tag{10d}$$

$$0 \leq E_{bt}^{s} \leq E_{b}^{cap} \tag{10e}$$

$$P_{bt}^{s} = P_{bt}^{Ds} - P_{bt}^{Cs} \tag{10f}$$

$$P_{bt}^{s} - P_{b,t-1}^{s} \leq P_{bt}^{Vs} \tag{10g}$$

$$P_{b,t-1}^{s} - P_{bt}^{s} \leq P_{bt}^{Vs} \tag{10h}$$

$$E_{b}^{min} - E_{bt}^{s} \leq E_{bt}^{EX,s} \tag{10i}$$

$$E_{bt}^{s} - E_{b}^{max} \leq E_{bt}^{EX,s} \tag{10j}$$

$$\forall b \in \mathcal{B}, \quad t \in \mathcal{T} \setminus 0, \; s \in \mathcal{S}$$

Load/balance constraints for all second stage variables are represented in (11). The constraint (12) allows for PV curtailment less than its forecasted value P_{vt}^{Fs}. Note that P_{vt}^{Fs} is the expected value of PV power for each scenario s for every time period t.

$$\sum_{g \in \mathcal{G}} P_{gt}^{s} + \sum_{b \in \mathcal{B}} P_{bt}^{s} + \sum_{v \in \mathcal{V}} P_{vt}^{s} = D_{t} - L_{t}^{s} \tag{11}$$

$$P_{vt}^{s} \leq P_{vt}^{Fs} \qquad \forall v \in \mathcal{V} \quad \forall s \in \mathcal{S}, t \in \mathcal{T} \setminus 0 \tag{12}$$

Finally, the total constraint set for our stochastic optimization combining the first and second stage is (4)–(12).

2.2 Scenario construction

As with any two-stage stochastic program, we need scenarios which will represent some random vector ξ which represents our PV scenarios and takes values $\xi^s = P_v^s$ for each scenario $s \in \mathcal{S}$. For one scenario, this vector represents a possible PV forecast for all 287 second stage time intervals for the representative test day. Recall that the first time interval represents present time, is in the first stage, and as such will use the measured PV value instead of forecasted scenarios. To construct all of the scenarios, we need a method of generating these possible PV forecasts. Fortunately, we already have PV forecasts from the winter, spring, and fall seasons for the real-world microgrid located in Hoover, Alabama. There were 196 days in total which had complete full-day forecast data available, with 86 of the days in the winter season, 54 days in spring, and 56 for fall. We will now describe how this collection of data was used to create full day samples of PV power forecasts, which were then used to create scenarios for the stochastic program.

The forecasts for the Hoover microgrid were provided by the Clean Power Research company, and contain 48 data points, one for each 30 minutes. An updated forecast is also issued every 30 minutes throughout the day. Because the optimization runs in 5-minute time intervals, one 30 minute forecast point is representative of six 5-minute time intervals. Creating individual daily scenarios involves collecting the first point in the 30 minute forecast that was issued, and aggregating them into a full 5-minute forecast for each day with complete data. Then, for a given test day, we use that day's original PV forecast plus 9 additional forecasts which were generated using the same aggregating method as our scenario collection for the stochastic program. We settled on 10 scenarios as a sufficient balance between computational tractability and solution quality. Each individual scenario was given a probability 1/10, and chosen based on one of two methods which will now be described.

The first method was to randomly sample 9 days from the collection of forecasts in the same season as the test day. The second method involved taking each collection of forecasts for the three seasons, and grouping them into smaller clusters by the k-means clustering algorithm. The k-means clustering algorithm partitions data into k clusters for which the squared euclidean distance from each point to its corresponding cluster's centroid is minimized. There are many initialization methods, but we chose a random assignment of k clusters for which the initial means were calculated. The algorithm then alternates between assigning all points to the cluster which minimizes their squared euclidean distance, and updating centroids, until cluster assignments stagnate. Our PV forecast data was broken into 2–3 clusters per season using the k-means clustering algorithm. Then, for a given test day, the 9 additional scenario forecasts will be chosen randomly from the k-means cluster containing the test day. This way, scenarios will forecasts which most closely resemble the forecast for the test day, in the hopes that this will group days with similar weather patterns together for the scenarios.

3 Computational results

Next we will describe the computational test instances and results. We will consider deterministic versions of the model in order to form a comparison to the stochastic model developed in Sect. 2. The deterministic models contain the same constraints as the stochastic model, with the difference being there is only one scenario corresponding to the singular PV forecast given for the real-world microgrid under its normal operation.

3.1 Test cases

To formulate test cases, all days were gathered for which the microgrid recorded complete PV forecasts, PV measurements, and load measurements over the 24 h. Five of these days with complete measurements were randomly selected as the test days. The controllable generation devices in the Hoover microgrid are a 330kW PV system, a 400kW natural gas generator with a minimum power output of 100kW, and a battery storage system with a power output of 300kW and capacity of 680kWh. The battery minimum state of charge is set to 20%, while the maximum is 80%. This means the battery will only enter a state of charge of 0-20% or 80-100% in an emergency situation, and the optimization will incur a penalty for entering this state. The generator minimum up-time was set to 30 minutes, or 6 time intervals, to avoid fast cycling of commitment status.

Four rolling time models were tested in total; two deterministic and two stochastic variants. The first case, referred to as (DM)is the deterministic model with the PV forecast D_t in (6) and (11) completely replaced with measured PV data for the test day. The other rolling deterministic model tested was simply using the singular PV forecast corresponding to the test day, and will be referred to as (DF). An example of the measured PV data versus deterministic forecast data for December, 23, 2018 is shown in Fig. 2. It can be observed that December 23 was an overcast day, as the maximum measured PV power output was around 140kW out of a total capacity of 330 kW.

For the two stochastic models, we first considered the stochastic model with seasonal data sampling (SSE), where 9 randomly sampled days from the same season as the test day were chosen. The last model is the stochastic model with scenarios

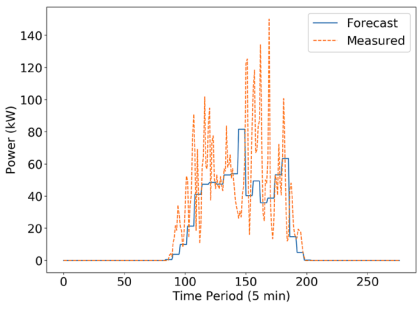

Fig. 2 PV forecast and measured values for 12/23/18

constructed by taking 9 days from the same k-means cluster as the test day (SKM). Recall that the PV forecast for the test day is used as the 10th scenario for each stochastic instance.

Also, we must recall that to simulate the real-world operation of the microgrid, the first stage will always represent the setpoints sent to the generation devices under realization of PV output. To accomplish this, the first time period in the PV forecast will always be replaced with the measured PV power value collected from the actual operation of the microgrid, as the optimization rolls through the day, per constraint (7).

To facilitate comparison with perfect information, we take use of the fact that measured PV values are available for the days we are testing. A fifth deterministic model was tested without rolling time, and with perfect information, referred to as PERF. When the rolling time models start, their forecast horizon is 24 h, as shown in Fig. 3. After rolling through all 24 h, the forecast horizon is now 48 h into the future from the original $t = 0$ at the initialization of the model. Therefore, we run the perfect information case PERF with a 48 h horizon, also demonstrated in Figure 3. However, while we minimize over all 48 h of operational cost, we report the cost for the first 24 h, as this will be comparable to the cost after the rolling horizon models have made it through 24 h of realization.

3.2 Results

The models were coded in python using the Pyomo modeling language [28, 29], and solved with Gurobi Version 8.1.0 on a 2x Intel E5-2670 CPU @ 2.6 ghz (16 cores, 32 threads total), with Ubuntu server 18.04 and 256GB ram. During simulation a mip gap of 2% was used in order to ensure adequate computation time in the stochastic cases. It is desirable for the models to solve within 5 minutes, as that is the length of the time intervals in this study. The extensive form solution for the stochastic models was found to solve in less than a minute for a majority of the solves, due to its relatively small size. In fact, only 27 of 1440 runs, less than 2%, exceeded

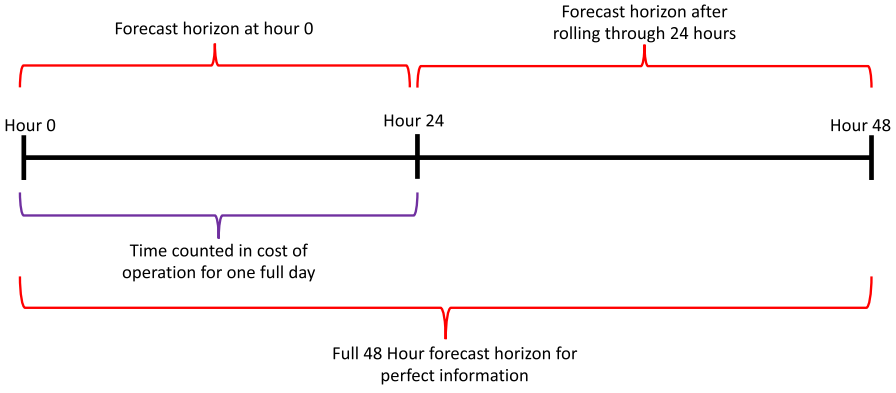

Fig. 3 Forecast Horizons for the Rolling Time and Perfect Information Models

the 5-minute window, and all were from the March 3rd 2019 test. If a solution hit max time, the best found solution at that time was used, and the computation was rolled to the next time interval. Because 98% of the the stochastic cases solved in under 5 minutes, advanced techniques such as progressive hedging [9] were not necessary. The deterministic models solved generally in no more than a few seconds.

Table 1 displays the cost of operation for the microgrid for each model after rolling through a full day on the rolling horizon models, and a full day cost for the PERF model (perfect information). For the rolling horizon models, the cost of operation at the first stage (t=0) is added together after each solve, creating the daily cost of operation as each time interval is realized. Recall that the PERF case is a one-shot optimization where the cost of operation is collected for the first 24 h. This is the same cost of operation window as the rolling time horizon models, with the exception that it is solved once instead of gathering one time period at a time.

The computational results present two interesting insights. That the DM out performs DF is to be expected, as they are both deterministic problems with DM using perfect information while DF relies on imperfect forecasted information. However, it does seem surprising that the difference between deterministic models is small. In addition, one would expect that stochastic models would under perform DM. This is especially true when considering neither of the stochastic models are particularly sophisticated. However in half of the cases, the stochastic models give cheaper solutions than the DM model. We argue that explanation for this behaviour is that end of horizon affects are driving the cost more than the uncertainty present in the microgrid, and that the benefit of the stochastic models is in their ability to provide a much better hedge for events that occur after the 24 h planning horizon.

Microgrids will certainly see a lot of variability in the areas of production (wind and PV) as well as load. However, there is a lot of internal robustness in the design of a microgrid that allows it to implicitly dampen the effect of this uncertainty. Any PV used in a residential microgrid will be sized in order to, more often that not, produce more during peak sun times than the neighborhood consumes during that period. Variability in the PV produced in a five minute intervals can easily be absorbed by the battery. Of more importance is variable of total daily PV production, but low total production can be overcome by running the generator. While not accounted for in this model, residential microgrids have even more tools to improve robustness. Changing HVAC set points to increase/decrease temporary demand can be used as a backup measure if the battery is unable to adapt to incorrect forecasts [30]. In addition, gas generators will likely be sized to be able to single

Table 1 Cost of operation in $ for each test case

Date	11/09/18	12/23/18	01/04/19	01/21/19	03/25/19
DM	235.27	366.64	277.12	565.85	109.96
DF	247.91	367.92	287.74	578.95	133.23
SSE	213.26	360.27	250.69	583.06	118.19
SKM	213.62	365.6	305.75	578.74	111.0
PERF	197.39	351.91	246.0	494.13	65.04

handedly cover most loads, so generators will almost always contribute to the battery whenever they turned used. Waiting until they are absolutely necessary, then using excess generation to power the battery, is a reasonably strategy for dealing with uncertainty. This natural resilience to uncertainty is magnified when one considers that residential microgrids are likely to be oversized, containing more PV and energy storage capability than is necessary for all but the most extreme days. This is certainly true in the Hoover, Al. where the battery is large enough to cover a typical load for 6–8 h all by itself. Continually re-optimizing the schedule in 15 minute intervals allows for the microgrid to take advantage of these resource, and in itself acts as a mitigator of uncertainty.

While incorporating uncertainty doesn't provide a significant impact on savings, the data does suggest that the length of the planning horizon can have a significant impact on overall costs. Recall that PERF looks at a two day planning horizon while the other methods do a one day rolling horizon. Using this schedule, based on a much larger planning horizon, provided far cheaper schedules than the alternative models. Given the need for fast solutions to fit real time operations, it seems that focusing on longer time horizons will yield better solutions than trying to incorporate uncertainty.

4 Conclusion

This work investigated the impact of stochastic approaches to microgrid scheduling. We use real data from a residential microgrid in Hoover, AL. to demonstrate that stochastic approaches are not likely to produce significant cost savings over deterministic methods, even when the error associated with solar forecasts is high. This is in part due to the rolling time horizon approach's ability to adjust to sudden changes as well as the natural robustness of the microgrid design. Given that solutions must be obtained quickly in a (near) real-time use, we argue that using longer time horizons in a derministic model are likely to be more impactful than incorporating uncertainty.

References

1. Bie, Z., Zhang, P., Li, G., Hua, B., Meehan, M., Wang, X.: Reliability evaluation of active distribution systems including microgrids. IEEE Trans. Power Syst. **27**(4), 2342 (2012)
2. Hatziargyriou, N., Asano, H., Iravani, R., Marnay, C.: Microgrids. IEEE Power Energy Mag **5**(4), 78 (2007)
3. D.E. Olivares, C.A. Ca nizares, M. Kazerani, A centralized energy management system for isolated microgrids, IEEE Trans Smart Grid **5**(4), 1864 (2014)
4. Hatziargyriou, N.: Microgrids: architectures and control. Wiley, Hoboken (2014)
5. Moretti, L., Astolfi, M., Vergara, C., Macchi, E., Pérez-Arriaga, J.I., Manzolini, G.: A design and dispatch optimization algorithm based on mixed integer linear programming for rural electrification. Appl. Energy **233**, 1104 (2019)
6. Zia, M.F., Elbouchikhi, E., Benbouzid, M.: Microgrids energy management systems: A critical review on methods, solutions, and prospects. Appl. Energy **222**, 1033 (2018)
7. Van Slyke, R.M., Wets, R.: L-shaped linear programs with applications to optimal control and stochastic programming. SIAM J. Appl. Math. **17**(4), 638 (1969)
8. Geoffrion, A.M.: Generalized benders decomposition. J. Optim. Theory Appl. **10**(4), 237 (1972)

9. Rockafellar, R.T., Wets, R.J.B.: Scenarios and policy aggregation in optimization under uncertainty. Math. Oper. Res. **16**(1), 119 (1991)
10. CarøE, C.C., Schultz, R.: Dual decomposition in stochastic integer programming. Oper. Res. Lett. **24**(1–2), 37 (1999)
11. Mulvey, J.M., Ruszczyński, A.: A new scenario decomposition method for large-scale stochastic optimization. Operat. Res. **43**(3), 477 (1995)
12. Hytowitz, R.B., Hedman, K.W.: Managing solar uncertainty in microgrid systems with stochastic unit commitment. Electr. Power Syst. Res. **119**, 111 (2015)
13. Mohammadi, S., Soleymani, S., Mozafari, B.: Scenario-based stochastic operation management of microgrid including wind, photovoltaic, micro-turbine, fuel cell and energy storage devices. Int. J. Electr. Power Energy Syst. **54**, 525 (2014)
14. Shen, J., Jiang, C., Liu, Y., Wang, X.: A microgrid energy management system and risk management under an electricity market environment. IEEE Access **4**, 2349 (2016)
15. Asensio, M., Contreras, J.: Stochastic unit commitment in isolated systems with renewable penetration under cvar assessment. IEEE Trans. Smart Grid **7**(3), 1356 (2015)
16. Farzin, H., Fotuhi-Firuzabad, M., Moeini-Aghtaie, M.: Stochastic energy management of microgrids during unscheduled islanding period. IEEE Trans. Ind. Inform. **13**(3), 1079 (2016)
17. Mazidi, M., Zakariazadeh, A., Jadid, S., Siano, P.: Integrated scheduling of renewable generation and demand response programs in a microgrid. Energy Convers. Manag. **86**, 1118 (2014)
18. Rezaei, N., Kalantar, M.: Stochastic frequency-security constrained energy and reserve management of an inverter interfaced islanded microgrid considering demand response programs. Int. J. Electr. Power Energy Syst. **69**, 273 (2015)
19. Zakariazadeh, A., Jadid, S., Siano, P.: Smart microgrid energy and reserve scheduling with demand response using stochastic optimization. Int. J. Electr. Power Energy Syst. **63**, 523 (2014)
20. D.E. Olivares, J.D. Lara, C.A. Ca nizares, M. Kazerani, Stochastic-predictive energy management system for isolated microgrids, IEEE Trans. Smart Grid **6**(6), 2681 (2015)
21. Su, W., Wang, J., Roh, J.: Stochastic energy scheduling in microgrids with intermittent renewable energy resources. IEEE Trans. Smart Grid **5**(4), 1876 (2013)
22. Palma-Behnke, R., Benavides, C., Lanas, F., Severino, B., Reyes, L., Llanos, J., Sáez, D.: A microgrid energy management system based on the rolling horizon strategy. IEEE Trans. Smart Grid **4**(2), 996 (2013)
23. Silvente, J., Kopanos, G.M., Dua, V., Papageorgiou, L.G.: A rolling horizon approach for optimal management of microgrids under stochastic uncertainty. Chem. Eng. Res. Des. **131**, 293 (2018)
24. J. Silvente, G.M. Kopanos, E.N. Pistikopoulos, A. Espu na, A rolling horizon optimization framework for the simultaneous energy supply and demand planning in microgrids, Appl. Energy **155**, 485 (2015)
25. McIlvenna, A., Ostrowski, J., Herron, A., King, D., Irminger, P., Hambrick, J., Ollis, B.: Practice summary: Improved reliability via optimization in residential microgrids. INFORMS J. Appl. Anal. **50**(2), 112 (2020)
26. A. McIlvenna, A. Herron, J. Hambrick, B. Ollis, J. Ostrowski, Reducing the computational burden of a microgrid energy management system, Comput. Ind. Eng. 106384 (2020)
27. Xu, B., Oudalov, A., Ulbig, A., Andersson, G., Kirschen, D.S.: Modeling of lithium-ion battery degradation for cell life assessment. IEEE Trans. Smart Grid **9**(2), 1131 (2016)
28. W.E. Hart, C.D. Laird, J.P. Watson, D.L. Woodruff, G.A. Hackebeil, B.L. Nicholson, J.D. Siirola, *Pyomo–optimization modeling in python*, vol. 67, 2nd edn. (Springer Science & Business Media, 2017)
29. Hart, W.E., Watson, J.P., Woodruff, D.L.: Pyomo: modeling and solving mathematical programs in python. Math. Program. Comput. **3**(3), 219 (2011)
30. Sharma, I., Dong, J., Malikopoulos, A.A., Street, M., Ostrowski, J., Kuruganti, T., Jackson, R.: A modeling framework for optimal energy management of a residential building. Energy Build. **130**, 55 (2016)